*Int. J. Electrochem. Sci.*, 17 **(2022)** Article Number: 221253, doi: 10.20964/2022.12.53

International Journal of
ELECTROCHEMICAL
SCIENCE
www.electrochemsci.org

*Short Communication*

# A Comparison of Vertical Electro-Gas Welding and Submerged arc Welding Methods on the Corrosion Behaviors of Crude Oil Storage Tank Steel in Simulated Seawater

*Cao Wang*[1], *Yuanyuan Li*[2], *Yang Liu*[1], *Chao Cheng*[1], *Changan Tian*[1], *Qiongyu Zhou*[2]

[1] School of Chemistry and Civil Engineering, Shaoguan University, Shaoguan 512005, Guangdong, China
[2] School of Materials Science and Energy Engineering, Foshan University, Foshan 528000, China
[*]E-mail: wangcao@mail.nwpu.edu.cn; zhouzhouqiongyuxf@126.com

*Received:* 1 October 2022 / *Accepted:* 14 November 2022 / *Published:* 30 November 2022

Large crude oil storage tanks (LCOSTs) are generally fabricated by high strength low alloy (HSLA) steels via welding process. In this paper, a comparison of vertical electro-gas welding (VEGW) and submerged arc welding (SAW) methods on the corrosion behaviors of HSLA steels in simulated seawater has been investigated by open circuit potential (OCP) monitoring, potentiodynamic polarization test, electrochemical impedance spectroscopy (EIS) measurement. Results reveal that the welding process would decrease the corrosion resistance of HSLA steel, and the VEGW joint shows better corrosion resistance than SAW joint, due to the nobler OCP values, decreased corrosion current density, lesser impedance value (|Z|) and smaller weight loss. The corrosion products formed on the surface VEGW joint are more compact than SAW joint, which can account for the fact that the VEGW joint owns better corrosion resistance than SAW joint.

**Keywords:** Vertical Electro-Gas Welding, Submerged arc Welding, Corrosion, Crude Oil Storage Tank Steel

## 1. INTRODUCTION

Energy is a necessary input for human development, social development, and economic growth [1]. Recently, the energy shortage problem caused by the rapid development of industries and changes of people's lifestyles disturbs the whole world [2]. Fossil fuel has been considered as the important strategic resource, because it remains the major energy source in most countries until now [3-4].

To rise the ability of tackling emergencies caused by unforeseen supply disruptions, establishment of national petroleum strategic reserve is imperative for a mature country [5]. Generally, the crude oil in reserve would be stored in the large crude oil storage tanks (LCOST), which is located near the harbor for the convenience of transportation [6]. As well known to all, the moist atmosphere

near harbor contains affluent chlorine [7]. In addition, the domestic crude oil mainly comes from the ocean or Middle East, which contains many chloride ions [8, 9]. Therefore, the corrosion problems of LCOSTs caused by chloride have been attracted more and more attentions [10, 11].

Most of LCOSTs are composed of the high strength low alloy (HSLA) steels via welding process [10, 12]. The welded joints are very critical for the mechanical property and corrosion resistance of the LCOSTs, due to the phase transformations in the fusion zone (FZ) and heat effect zone (HAZ) introduced by the residual stresses and metallurgical changes [13-16]. That to say, an optimal welding technology can provide good corrosion resistance for LCOSTs [17]. However, the research on the corrosion behavior of welded joints is still limited, especially that in the seawater.

In this paper, a comparison of vertical electro-gas welding (VEGW) and submerged arc welding (SAW) methods on the corrosion behaviors of crude oil storage tank steel in simulated seawater has been investigated by a series of electrochemical technologies, such as open circuit potential (OCP) monitoring, potentiodynamic polarization curve, electrochemical impedance spectroscopy (EIS).

## 2. EXPERIMENTAL

The HSLA steels (API-5L X80) used in this work were drawn from a LCOST. The chemical composition (wt. %) is 0.09 C, 1.39 Mn, 0.007 Ti, < 0.004 S, < 0.004 P, bal. Fe. The VEGW joint was produced by single-pass welding, and the SAW joint was fabricated by multi-pass welding. The established suitably welding parameters are listed in Table 1.

**Table 1** The welding parameters for preparing VEGW joint and SAW joint

| Mode | Current (A) | Voltage (V) | Speed (cm/min) | heat input (KJ/cm) |
|---|---|---|---|---|
| VEGW | 450 | 45 | 12 | 100 |
| SAQ | 500 | 30 | 40 | 30 |

The samples with the dimension of 10 mm×10 mm×4 mm for electrochemical tests were machined by electrical discharge machining followed by grinding and polishing. Then, the samples were embedded in an epoxy resin to retain an exposed area of 1 $cm^2$. Electrochemical tests were performed on an electrochemical workstation (CHI660D) with a three-electrode cell, containing a platinum sheet (20×20 mm) as counter electrode, a saturated calomel electrode (SCE) as reference electrode and the prepared samples as working electrode. All electrochemical tests were carried out in an artificial seawater prepared according to the standard ASTM D1141-98 (2013) , which contains 24.53 g/L NaCl, 5.2 g/L $MgCl_2$, 4.09 g/L $Na_2SO_4$, 1.16 g/L $CaCl_2$, 0.6953 g/L KCl, 0.201 g/L $NaHCO_3$, 0.101 KBr, 0.027 g/L $H_3BO_3$, 0.025 g/L $SrCl_2$, 0.003 g/L NaF. All the tests were carried out at ~25 $^oC$, open to air.

The open circuit potentials (OCP) were recorded during the immersion period. In addition, the potentiodynamic polarization tests were scanned from -0.85 V to -0.55 V at a scan rate of 1 mV/s. The

EIS measurements were carried out at OCP from $10^5$ Hz to $10^{-2}$ Hz with a sinusoidal potential amplitude of 10 mV.

Five replicate samples (exposed surface is 2 $cm^2$) were immersed in artificial seawater solution by means of nylon wires for 90 days to measure the weight loss. During the immersion period, the artificial seawater solution was open to air and deionized water was added to maintain the solution concentration. After immersion, the corroded samples were immersed in 37% HCl solution about 30 s to remove oxides (or other corrosion products). Then, the samples were washed by rinsing in ultrapure water and ethanol, followed by blow-dry using cold-blast air. Finally, the weight of the sample was measured and recorded. The weight loss should be the results of original weight subtract the recorded weight. Moreover, the morphologies and structure of the corrosion products of sample surface after immersed for 90 days were examined by a scanning-electron microscope (SEM, JEOL JSM-6700F, operating at 15 kV) and an X-Ray diffractometer (XRD, D/max-2200) using the Cu K-alpha radiation ($\lambda$ = 1.5406 Å, operating at 40 kV and 200 mA).

## 3. RESULTS AND DISCUSSION

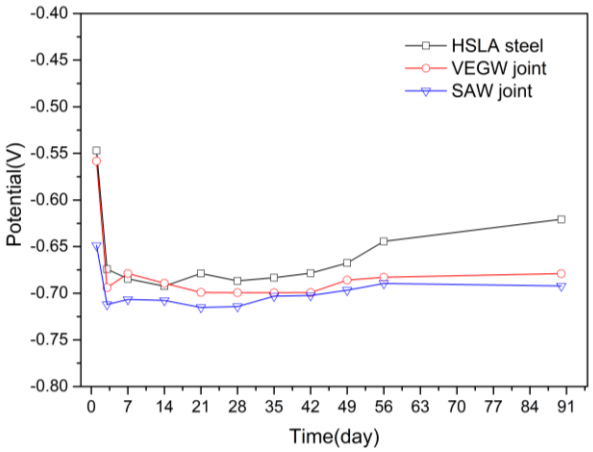


**Figure 1.** OCP versus time for HSLA steel, VEGW joint and SAW joint immersed in simulated seawater

Fig. 1 show the OCP versus time for HSLA steel, VEGW joint and SAW joint, which the testing medium is simulated seawater, immersion time is 90 days. It is clearly that the OCP values decrease significantly in the initial period of immersion (< 7days). This phenomenon would be attributed to be the fact that the oxides formed in ambient air are destroyed in the simulated seawater [18, 19]. After 7day of immersion, the OCP values would tend to be stable, because the dynamical equilibrium between the formation and dissolution of the oxides has been achieved [20]. In addition, it can be found that the OCP value decreases in the order: HSLA steel> VEGW joint>SAW joint. It means that the long-term stability of welding joints are worse than of HSLA steel, and the VEGW joint has better corrosion resistance than SAW joint.

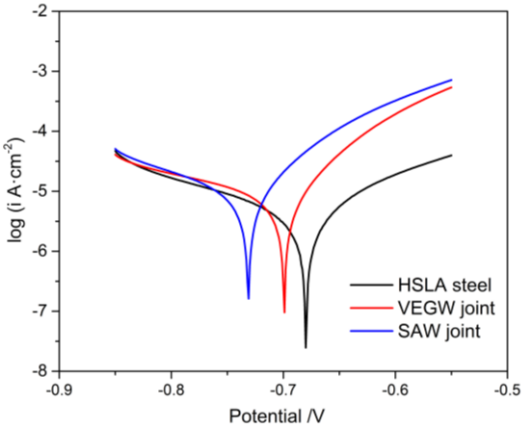


**Figure 2.** Potentiodynamic polarization curves of HSLA steel, VEGW joint and SAW joint in simulated seawater

Fig. 2 shows the potentiodynamic polarization curves of HSLA steel, VEGW joint and SAW joint in the simulated seawater. The corresponding corrosion parameters extracted from the polarization curves are listed in Table 2. Clearly, the HSLA steel owns nobler corrosion potentials ($E_{corr}$) than VEGW joint and SAW joint, and the corrosion current density ($i_{corr}$) decrease in the order: SAW joint > VEGW joint> HSLA steel, which confirms that the welding will decrease the corrosion resistance of HSLA steel In the case of two welding joints, the VEGW shows better performance in corrosion resistance than SAW [21].

**Table 2.** The electrochemical parameters extracted from the polarization curves in Figs. 2.

| Samples | $E_{corr}$ (mV) | $i_{corr}$ (μA·cm$^{-2}$) |
|---|---|---|
| HSLA steel | -679 | 1.6 |
| VEGW joint | -696 | 3.4 |
| SAW joint | -730 | 3.9 |

To investigate the corrosion behaviors at the electrode/electrolyte interface of the HSLA steel, VEGW joint and SAW joint in the simulated seawater, the EIS measurement, a typical non-destructive electrochemical technique, was performed during the whole immersion period [22]. The obtained EIS spectra were displayed in Fig. 3. With the prolongation of immersion time, the values of impedance (|Z|) increase (Fig. 3a, Fig. 3c and Fig. 3e), due to the generation of more oxides on the surface and shielding part of the exposed metal matrix. In addition, the VEGW joint shows bigger |Z| than SAW joint at the same immersion time. In addition, there exists a time constant at higher frequencies for all samples form the phase angle-frequency bode plots showed in Fig. 3b, Fig. 3d and Fig. 3f. This time constant can describe the characteristic of the formed compact oxide/corrosion products on the surface [23]. The time constant at intermediate frequencies region tend to trail off as the increase of immersion time, notarizing that the oxide/corrosion products become much denser [24].

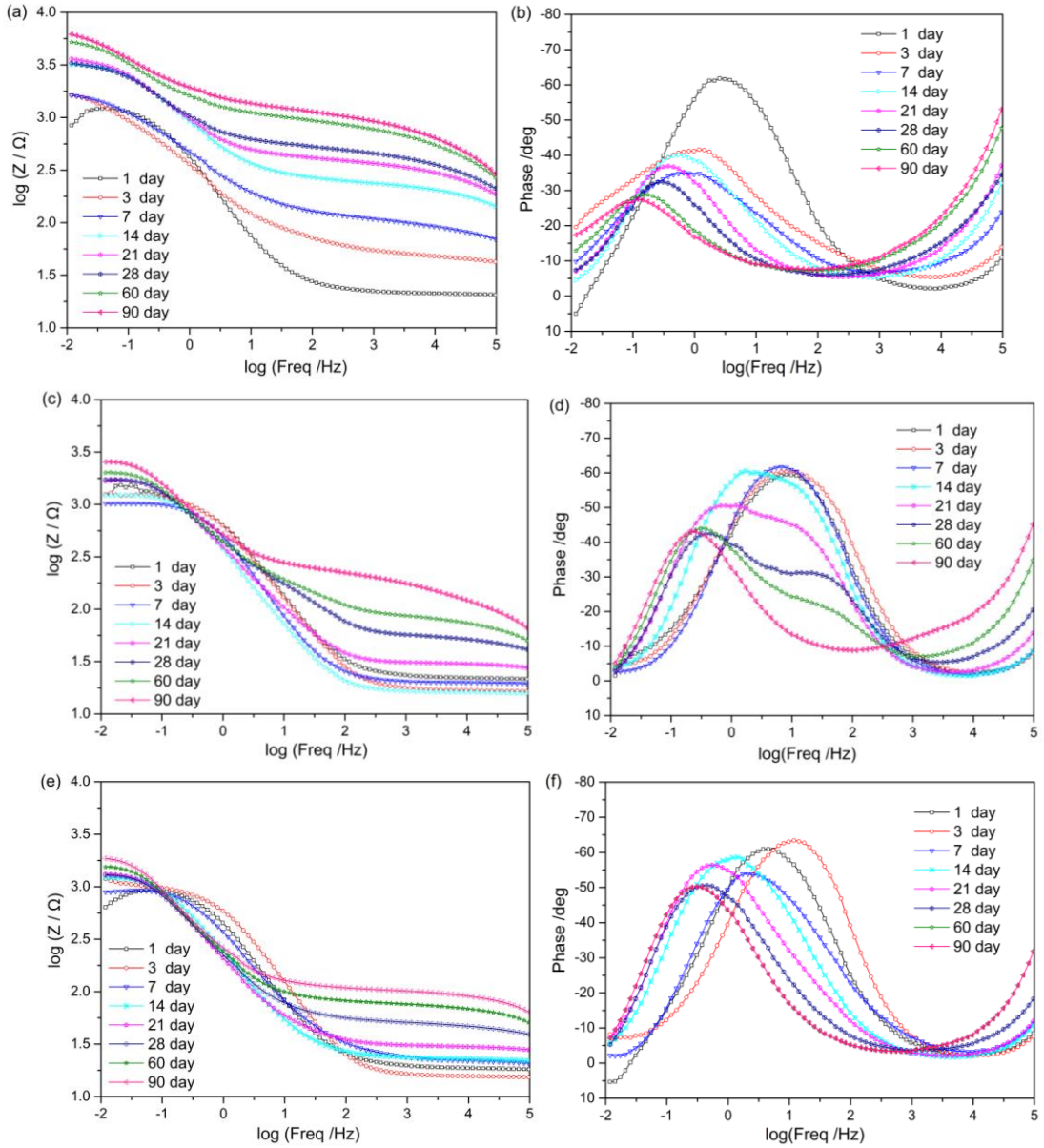


**Figure 3.** EIS spectra of different specimens immersed in simulated seawater (a-b: HSLA steel; c-d: VEGW joint; e-f: SAW joint)

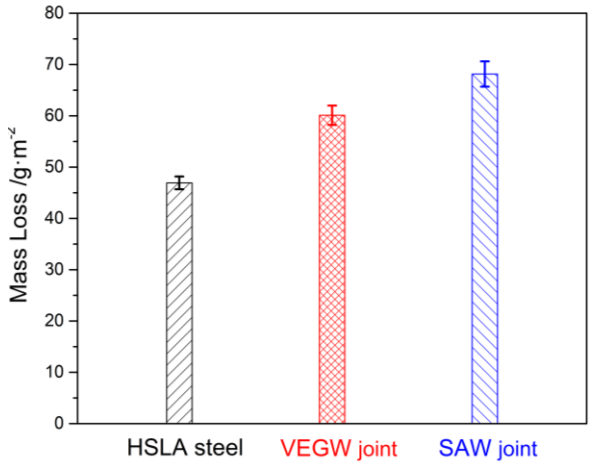


**Figure 4.** Mass loss of different samples immersed in simulated seawater for 90 days

Fig. 4 exhibits the average values of weight loss of different samples immersed in simulated seawater for 90 days. The weight loss is in the order: SAW joint > VEGW joint> HSLA steel. This result is highly in correspondence with the corrosion electrochemical test results, such as potentiodynamic polarization curves and EIS plots.

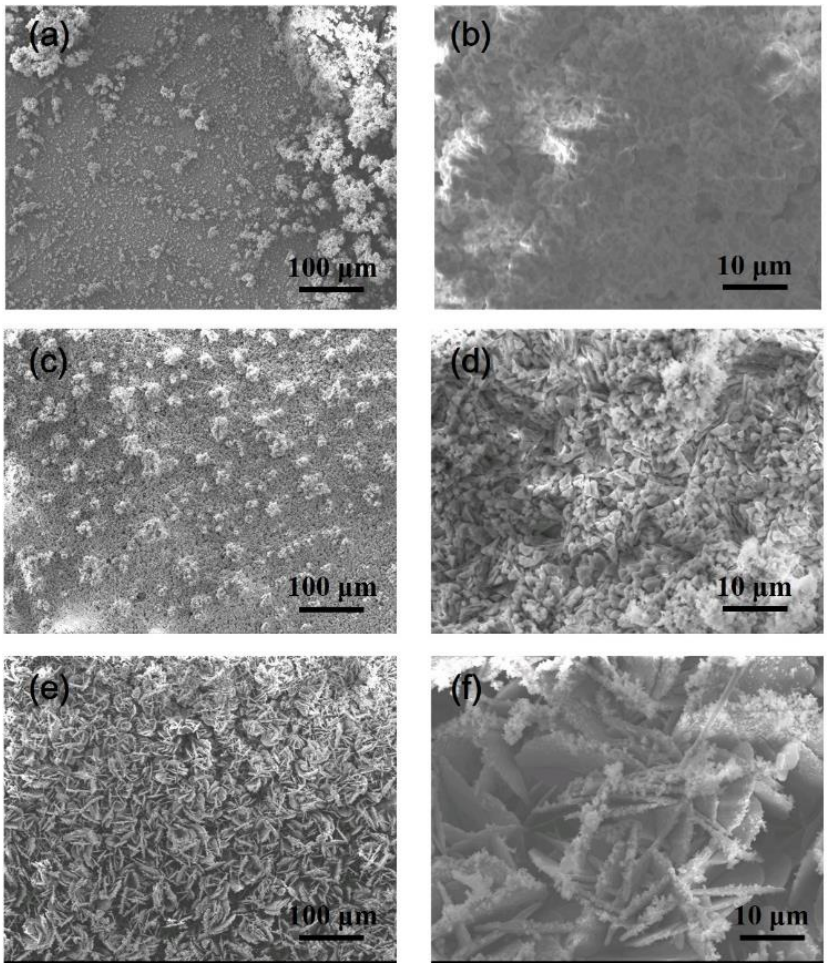


**Figure 5.** SEM morphologies of the specimen surfaces after immersed in simulated seawater for 90 days (a-b: HSLA steel; c-d: VEGW joint; e-f: SAW joint)

Fig. 5 shows the SEM morphologies of the specimen surfaces after immersed in simulated seawater for 90 days. Obviously, the corrosion products formed on the surface of HSLA steel are quite homogeneous and compact, while that formed on the surface of VEGW joint and SAW joint are less compact. Furthermore, a number of pores can be observed on the surface of VEGW joint and SAW joint, which can act as transmission channels for corrosive ion. Particularly, the corrosion products on the surface of SAW joint are primary consist of lamellar structure, resulting in a large number of pores.

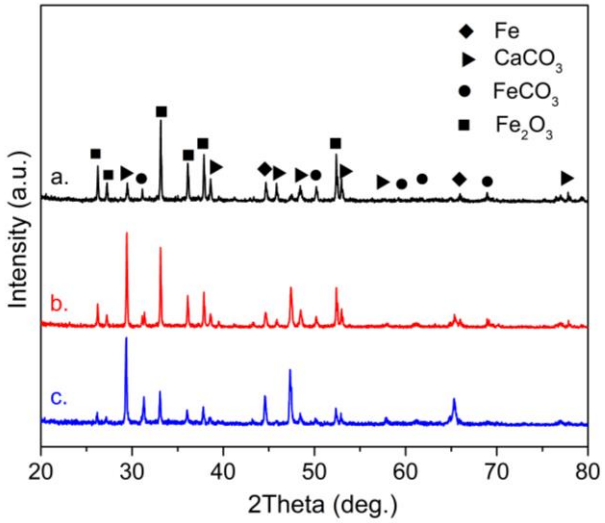


**Figure 6.** XRD patterns of different specimens after immersed in simulated seawater for 90 days (a: HSLA steel; b: VEGW joint; c: SAW joint)

Fig. 6 shows the XRD patterns of the specimens after immersed in simulated seawater for 90 days. As shown, three specimens display the similar XRD result, and the corrosion products are mainly composed of $Fe_2O_3$, $FeCO_3$ and $CaCO_3$. Besides, the diffraction peaks of Fe phase were found in the XRD patterns, which should be ascribed to the uncovered substrate. which should be ascribed to the uncovered substrate. In addition, it can be observed that the diffraction peak intensity of $Fe_2O_3$ are in the order: HSLA steel > VEGW joint > SAW joint, and the diffraction peak intensity of $FeCO_3$ and $CaCO_3$ are in the order: HSLA steel < VEGW joint < SAW joint. Generally, the compact corrosion products of $Fe_2O_3$ can be possibly generated on the surface of steel in the corrosive solution and then restrained the general corrosion [25, 26]. While the existence of carbonas ($FeCO_3$ and $CaCO_3$) would reduce the compactness of corrosion products and decrease the corrosion protection effects [27].Therefore, the corrosion products of VEGW joint contain more compact $Fe_2O_3$ and less $FeCO_3$ and $CaCO_3$ than that of SAW joint, which once again demonstrate the better corrosion resistance of the former than the latter. This result can provide the basis for ascertain of welding method for LCOST to meet the challenge of corrosion.

## 4. CONCLUSION

In this paper, the corrosion behaviors of HSLA steel, VEGW joint and SAW joint have been investigated by OCP monitoring, potentiodynamic polarization curve, EIS and weight loss experiment. From the obtained experimental results, following conclusions can be drawn:

(1) The OCP values decrease significantly in the initial period of immersion (＜7days) and then tend to be stable at the later stage. In addition, the VEGW joint exhibits nobler OCP value than SAW joint.

(2) The corrosion current density ($i_{corr}$) decrease in the order: SAW joint > VEGW joint> HSLA steel.

(3) With the prolongation of immersion time, the values of impedance increase for all samples. Besides, the VEGW joint shows bigger |Z| than SAW joint at the same immersion time.

(4) The weight loss are in the order: SAW joint > VEGW joint> HSLA steel.

(5) The corrosion products of VEGW joint contain more compact Fe2O3 and less FeCO3 and CaCO3 than that of SAW joint, resulting the more compact corrosion products and better corrosion resistance.

ACKNOWLEDGEMENTS
This work is financially supported by the Key Scientific and Technological Project of Foshan City (1920001000409) and Guangdong Basic and Applied Basic Research Foundation (No.2021A1515010671, 2020A1515011221), Guangdong Province Key Construction Discipline Scientific Research Ability Promotion project (No.2021ZDJS071), Natural Science Foundation of Shaoguan University (No.SZ2020KJ03), Characteristic innovation Projects of Colleges and Universities in Guangdong Province (No.2021KTSCX122, 2022KQNCX077)..

## References

1. B. Lin and B. Xu, Sci. *Total Environ.*, 719 (2020) 137503.
2. S. Dharma, H.C. Ong, H.H. Masjuki, A.H. Sebayang and A.S. Silitonga, *Energy Convers. Manag.,* 128 (2016) 66–81.
3. P.K. Sahoo, L.M. Das, M.K.G. Babu and S.N. Naik, *Fuel,* 86 (2007) 448–454.
4. A. Buasri, N. Chaiyut, V. Loryuenyong, P. Worawanitchaphong and S. Trongyong, *Sci. World J.,* 2013 (2013) 1–8.
5. C. Difiglio, *Energy Strateg. Rev.,* 5 (2014) 48-58.
6. H. Zhang, Y. Liang, Q. Liao, J. Gao, X. Yan and W. Zhang, *Chem. Eng. Res. Des.,* 137 (2018) 434-451.
7. R.E. Melchers and R. Jeffrey, *Corros. Sci.*, 65 (2012) 26-36.
8. J.H. Ding, L. Zhang and X.M. Lu, *Appl. Surf. Sci.*, 289 (2014) 33–41.
9. M.Ö. Öteyaka and H. Ayrtüre, *Int. J. Electrochem. Sci.*, 10 (2015) 8549-8557.
10. W. Liu, H. Pan, L. Li, H. Lv, Z. Wu, F. Cao and J. Zhu, *J. Manuf. Process*, 25 (2017) 418-425.
11. H. Tristijanto, M.N. Ilman and P.T. Iswanto, *Egypt. J. Pet.*, 29 (2020)155-162.
12. E. Olorundaisi, T. Jamiru, and A. T. Adegbola, *Mater. Res. Express*, 6 (2020) 1265k9.
13. R.S. Vidyarthy and D.K. Dwivedi, *J. Mater. Eng. Perform.*, 26 (2017) 5375-5384.
14. R. Unnikrishnan, K.S. Idury, T.P. Ismail, A. Bhadauria, S.K. Shekhawat, R.K. Khatirkar and S.G. Sapate, *Mater. Charact.*, 93 (2014) 10-23.
15. K.D. Ramkumar, P.S. Goutham, V.S. Radhakrishna, A. Tiwari and S. Anirudh, *J. Manuf. Process*, 23 (2016) 231-241.
16. K.D. Ramkumar, W.S. Abraham, V. Viyash, N. Arivazhagan and A.M. Rabel, *J. Manuf. Process,* 25 (2017) 306-322.
17. W.M. Liu, Q.J. Zhou, L.S. Li. *J. Alloys Compd.*, 598 (2014) 198–204.
18. L. Freire, M.J. Carmezim, M.G.S. Ferreira, M.F. Montemor, *Electrochim. Acta*, 56(2011) 5280.
19. L. Freire, M.A. Catarino, M.I. Godinho, M.J. Ferreira, M.G.S. Ferreira, A.M.P. Simões, M.F. Montemor, *Cement. Concrete. Comp.*, 34 (2012) 1075.
20. A. Gupta and C. Srivastava, *Corros. Sci.*, 194 (2022) 109945.

21. Q. Zhou, J. Jiang, Q. Zhong, Y. Wang, K. Li and H. Liu, *J. Alloy. Compd.*, 563 (2013) 171.
22. Q. Zhou, S. Liu, L. Gan, X. Leng and S. Wei. *Mater. Res. Express.*, 5 (2018) 116534
23. N.C. Rosero-Navarro, S.A. Pellice, A. Durán and M. Aparicio, *Corros. Sci.*, 50 (2008) 1283
24. S.S. Xin and M.C. Li. *Corros. Sci.*, 81 (2014) 96.
25. X. Chen, Z. Guan, M. Du and C. Lin. *Int. J. Electrochem. Sci.*, 14 (2019) 7332-7347.
26. F. Rubino, D. Merino, C. Munez and P. Poza. *Key Eng. Mater.*, 926 (2022) 1736-1745.
27. R.A. De Motte, R. Barker, D. Burkle, S.M. Vargas and A. Neville, *Mater. Chem. Phys.*, 216 (2018) 102-111.